THE JOURNAL OF BIOLOGICAL CHEMISTRY VOL. 285, NO. 24, pp. 18309–18318, June 11, 2010
© 2010 by The American Society for Biochemistry and Molecular Biology, Inc. Printed in the U.S.A.

Ribosomal 18 S RNA Processing by the IGF-I-responsive WDR3 Protein Is Integrated with p53 Function in Cancer Cell Proliferation*[S]

Received for publication, January 29, 2010, and in revised form, April 13, 2010 Published, JBC Papers in Press, April 14, 2010, DOI 10.1074/jbc.M110.108555

Mary McMahon[‡], Verónica Ayllón[‡], Kostya I. Panov[§], and Rosemary O'Connor[‡1]

From the [‡]Cell Biology Laboratory, Department of Biochemistry, BioSciences Institute, University College Cork, Cork, Ireland and the [§]School of Biological Sciences, Queen's University Belfast, Belfast BT9, 7BL Northern Ireland

Insulin-like growth factor-I (IGF-I) signaling is strongly associated with cell growth and regulates the rate of synthesis of the rRNA precursor, the first and the key stage of ribosome biogenesis. In a screen for mediators of IGF-I signaling in cancer, we recently identified several ribosome-related proteins, including NEP1 (nucleolar essential protein 1) and WDR3 (WD repeat 3), whose homologues in yeast function in ribosome processing. The *WDR3* gene and its locus on chromosome 1p12-13 have previously been linked with malignancy. Here we show that IGF-I induces expression of *WDR3* in transformed cells. WDR3 depletion causes defects in ribosome biogenesis by affecting 18 S rRNA processing and also causes a transient down-regulation of precursor rRNA levels with moderate repression of RNA polymerase I activity. Suppression of WDR3 in cells expressing functional p53 reduced proliferation and arrested cells in the G_1 phase of the cell cycle. This was associated with activation of p53 and sequestration of MDM2 by ribosomal protein L11. Cells lacking functional p53 did not undergo cell cycle arrest upon suppression of WDR3. Overall, the data indicate that WDR3 has an essential function in 40 S ribosomal subunit synthesis and in ribosomal stress signaling to p53-mediated regulation of cell cycle progression in cancer cells.

Ribosome biogenesis is a tightly regulated and complex process essential for development, growth, and cell cycle regulation (1, 2). Transcription of the 47 S rRNA precursor, a key step in ribosome synthesis, occurs in the nucleolus and is dependent on RNA polymerase I (pol I)[2] activity (3, 4). This precursor is processed by endo- and exonucleolytic cleavage mechanisms to generate the mature 18, 5.8, and 28 S rRNA (5). The processing of ribosomes is highly responsive to extracellular growth signals and constitutes a major energy-consuming process within cells (6). Thus, it is not surprising that the rate of ribosome biogenesis is tightly coordinated with cell growth and proliferation. Alterations to ribosome biogenesis often result in disruption to the cell cycle, mediated by the tumor suppressor protein p53 (7, 8).

Ribosome-induced nucleolar disturbance is thought to activate p53 by blocking proteasomal degradation via MDM2 (9, 10). This can be achieved by negative regulation of MDM2 by the tumor-suppressor protein p19ARF or ribosomal proteins, both of which can sequester MDM2 leading to stabilization of p53 (11–13). Recently, ribosomal protein (rp) L11 was found to bind MDM2 resulting in activation of p53 upon impairment of 40 S ribosome synthesis with no evident effect on nucleolar integrity (14), indicating that defects in ribosome biogenesis could trigger activation of the p53 stress response pathway in the presence or absence of intact nucleoli.

The IGF-I signaling pathway has a significant role in ribosome biogenesis. It enhances rRNA transcription by increasing the activity of the upstream binding factor (15, 16) and by increasing promoter occupancy with the essential core promoter-binding factor SL1 (17). Mouse embryonic fibroblasts derived from an IGF-I receptor (IGF-IR) knock-out mouse, R^- cells (18), exhibit slower growth rates, elongation of all stages of the cell cycle, and a decreased rate of ribosome synthesis in comparison with wild-type cells (19). However, there are no reports of IGF-I regulating the expression of proteins involved in ribosome biogenesis.

We recently carried out a functional screen to identify proteins associated with IGF-IR-mediated cellular transformation, which included several proteins involved in metabolism, such as the mitochondrial carrier PNC1 and the vacuolar H^+-ATPase regulator HRG-1 (20–22). Moreover, in this screen, a number of ribosomal proteins associated with both the large and small ribosomal subunit formation were identified. Two proteins with homologues involved in yeast 18 S rRNA synthesis, NEP1 and WDR3, were among this group. NEP1, also known as EMG1 (essential for mitotic growth 1), is essential for the biogenesis of 18 S rRNA and 40 S ribosome synthesis in yeast (23, 24). WDR3 is a nuclear protein consisting of 10 WD repeat units. It is located on chromosome 1p12-p13 (25), at a region that is frequently altered in malignancies and solid tumors (26, 27). The yeast homologue of WDR3, Utp12, is a component of the pre-rRNA processing complex and is essential for rRNA processing and synthesis of the small ribosomal subunit (28). In this study we sought to determine how the

* This work was supported by Science Foundation Ireland, the Irish Research Council for Science, Engineering, and Technology, and the Health Research Board.

[S] The on-line version of this article (available at http://www.jbc.org) contains supplemental Figs. S1–S7.

[1] To whom correspondence should be addressed. Tel.: 353214901312; Fax: 353214901382; E-mail: r.oconnor@ucc.ie.

[2] The abbreviations used are: pol I, polymerase I; IGF-I, insulin-like growth factor-I; IGF-IR, IGF-I receptor; siRNA, small interfering RNA; siNEG, negative control siRNA; RT, reverse transcription; pre-rRNA, precursor rRNA; Rb, retinoblastoma protein; rp, ribosomal protein; mTOR, mammalian target of rapamycin; PI3K, phosphatidylinositol 3-kinase; FSC-H, forward scatter height; GAPDH, glyceraldehyde-3-phosphate dehydrogenase.

function of WDR3 in ribosome biogenesis affects the growth and proliferation of cancer cells.

MATERIALS AND METHODS

Cell Culture and IGF-I Stimulation—R^+, R^-, Rat-1, Rat-1/Myc, MCF-7, U2OS, SAOS-2, and HeLa cell lines were cultured in Dulbecco's modified Eagle's medium (supplemented with 10% fetal bovine serum, 20% fetal bovine serum for SAOS-2 cell line), 10 mM L-glutamine, and 5 mg/ml penicillin and streptomycin (all from Sigma). For IGF-I stimulations, R^+ and MCF-7 cells were serum-starved for 4 or 12 h, respectively, prior to stimulation with 100 ng/ml (or 10 ng/ml where indicated) IGF-I (PeproTech, Rocky Hill, NJ). All pharmacological inhibitors (20 μM LY294002, 20 nM rapamycin, and 30 μM PD98059) were from Calbiochem and were added 30 min prior to IGF-I stimulation.

Small Interfering RNA (siRNA) Transfection—Two pre-designed siRNA oligonucleotides specific for the human *WDR3* gene (siRNA A ID 136062 and siRNA B ID 136064) and negative control siRNA (siNEG) were obtained from Ambion (Austin, TX). Transfections were carried out with 10 nM oligonucleotides using Oligofectamine transfection reagent (Invitrogen) according to the manufacturer's instructions. Protein levels were assessed for WDR3 expression by Western blot analysis 48–72 h post-siRNA transfection.

Northern Blot and pre-rRNA Analysis—Total RNA from MCF-7 and U2OS cells was isolated using TRIzol (Invitrogen) according to the manufacturer's instructions. 20 μg (MCF-7 cells) or 10 μg (U2OS cells) of total RNA was separated on a 1% (w/v) agarose-formaldehyde gel and blotted onto Hybond N^+ membrane (GE Healthcare) followed by UV cross-linking (UV-Stratalinker 1800, Stratagene). Pre-hybridization and hybridization were carried out at 42 °C in 50% formamide, 5× SSC, 4× Denhardt's solution, 0.1% SDS for 2 and 16 h, respectively. For Northern blot analysis of *WDR3* expression, a probe spanning nucleotides 48–906 of *WDR3* cDNA was labeled with [α-^{32}P]ATP by the random primer method (NEBlot, New England Biolabs). Membranes were washed twice using 2× SSC, 0.1% SDS, for 5 min at 42 °C and twice using 0.5× SSC, 0.1% SDS for 15 min at 42 °C and then exposed to Storm PhosphorImager screen. rRNA precursors were visualized using DNA oligonucleotide (10 pmol) specific for human ITS-1, ITS-2, and 18 and 28 S as described (29). Oligonucleotides were end-labeled with [γ-^{32}P]ATP and T4 polynucleotide Kinase (New England Biolabs). Signal intensities from phosphorimages were quantified using ImageQuant TL software (Amersham Biosciences).

In Vitro Transcription Assays and pre-rRNA Level Determination—In vitro specific transcription reactions were performed as described previously (30, 31) at a final salt concentration of 50 mM KCl. The resulting transcripts were analyzed in an S1 nuclease protection assay after annealing the RNA to a 5′-end ^{32}P-labeled oligonucleotide, which was complementary to the region between +1 and +40 of 47 S pre-rRNA. Signals were quantified using Fuji PhosphorImager and Aida software. Nonspecific (promoter-independent and randomly initiated) transcription assay was performed as described previously (32). Total RNA and proteins were isolated using RNeasy kit (Qiagen) according to the manufacturer's instructions (only isolate RNA which is longer then 200 bp). pre-rRNA levels were determined by S1 nuclease protection assay (as above) using 5 and 10 μg of RNA per reaction.

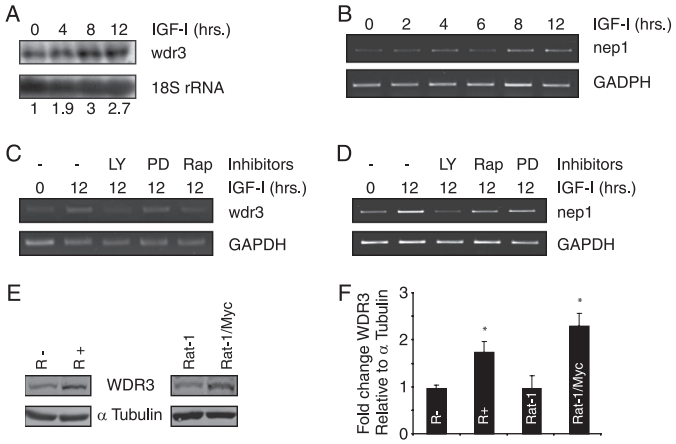

FIGURE 1. **IGF-I induces expression of *WDR3* and *NEP1* mRNA.** *A,* MCF-7 cells were serum-starved for 12 h and stimulated with 100 ng/ml IGF-I for the indicated time. Total RNA was extracted, and Northern blot analysis was performed using probes specific for *WDR3* and 18 S rRNA. Numerical values represent fold change *WDR3* mRNA expression relative to 18 S rRNA and normalized to expression at time 0 h. Results represent one of two independent Northern blotting experiments with similar results. *B,* MCF-7 cells were serum-starved for 12 h and stimulated with 100 ng/ml IGF-I for the indicated times. Total RNA was extracted and analyzed by semi-quantitative RT-PCR using *NEP1* and *GAPDH* primers. Results represent one of three independent experiments with similar results. *C,* MCF-7 cells were pre-treated with LY294002 (*LY*), rapamycin (*Rap*), and PD98059 (*PD*) for 30 min prior to IGF-I stimulation with 100 ng/ml IGF-I. Total RNA was extracted and analyzed by semi-quantitative RT-PCR using *WDR3* and *GAPDH* primers. Results represent one of three independent experiments with similar results. *D,* MCF-7 cells were treated as in *C*. Total RNA was extracted and analyzed by semi-quantitative RT-PCR using *NEP1* and *GAPDH* primers. Results represent one of three independent experiments with similar results. *E,* level of WDR3 protein was analyzed from protein lysates of R^+, R^-, Rat-1, and Rat-1/Myc cells by Western blot analysis using an antibody generated to detect WDR3. α-Tubulin was used as a loading control. Results represent one of five independent experiments with similar results. *F,* graph represents fold change WDR3 expression relative to α-tubulin normalized to levels in R^- or Rat-1 cells from three similar experiments to that shown in *E*. *, $p < 0.05$, Student's *t* test.

Western Blotting and Immunoprecipitation—Cells were lysed in 50 mM Tris-HCl, pH 8, 150 mM NaCl, 1% Nonidet P-40, 0.1% SDS, 0.5% sodium deoxycholate, 1 mM NaF, 1 mM phenylmethylsulfonyl fluoride, 1 mM sodium orthovanadate, 1 μM pepstatin, 1.5 μg/ml aprotinin (RIPA buffer). Cytoplasmic, soluble nuclear and insoluble nuclear extracts were prepared as described previously (33). Following separation in SDS-PAGE on 8 or 4–20% gradient gels, proteins were transferred to nitrocellulose membrane for Western blotting. Membranes were incubated overnight with the following primary antibodies: WDR3 polyclonal antibody (generated using a peptide corresponding to amino acids residues 114–127 of human and mouse WDR3 protein (KYDQLGGRLASGSK) (GenScript, NJ)); anti-WDR3 (Bethyl Laboratories, Inc.); anti-β-actin and anti-α-tubulin (both Sigma); anti-L11 (Invitrogen); anti-p53 (DO-1), anti-MDM2 (SMP14), anti-p21 (C-19), anti-lamin B (M-20), anti-RPA135 (N17) (all Santa Cruz Biotechnology); anti-poly(ADP-ribose) polymerase anti-p53 (1C12) and anti-phospho-Rb (Ser-780) (all Cell Signaling Technology); anti-polymerase I -associated factor 53 (PAF53) antibodies (Transduction Laboratories); and anti-β-actin-horseradish peroxidase

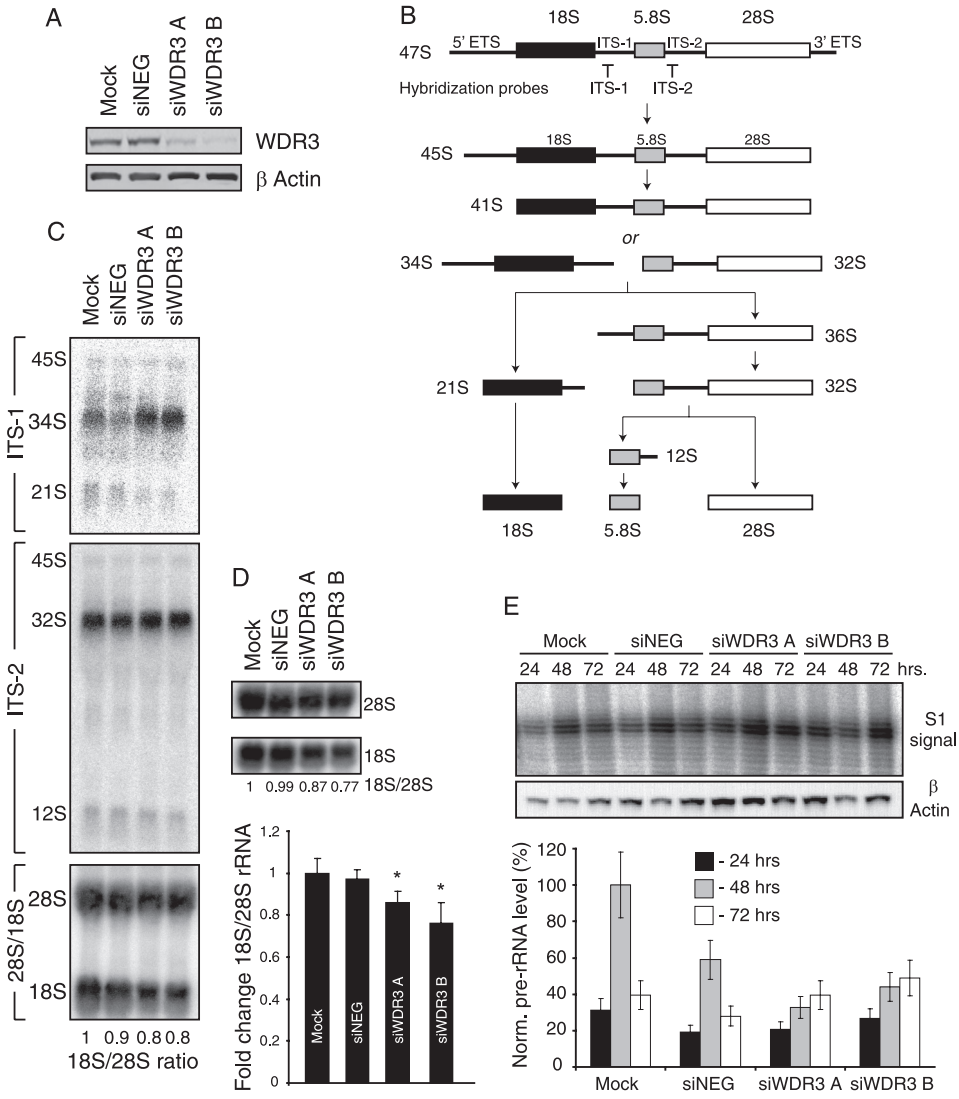

FIGURE 2. **WDR3 is required for rRNA processing.** *A,* U2OS cells were transfected with mock, control siRNA (siNEG), or two siRNA oligonucleotides targeting WDR3, siWDR3 A, and siWDR3 B. WDR3 protein levels were analyzed by Western blot analysis 72 h post-siRNA transfection using commercially available WDR3 antibody. β-Actin was used as a loading control. Data shown indicate WDR3 protein levels in cells used in *C* and represent one of three independent experiments with similar results. *B,* schematic diagram representing the primary 47 S rRNA transcript and mammalian rRNA processing pathways, with the position of hybridization probes shown. *C,* total RNA from U2OS cells transfected with mock, control siRNA (siNEG), or siRNA targeting WDR3 was analyzed by Northern blotting for rRNA species using probes specific for human ITS-1, ITS-2, and 28 and 18 S rRNA. Ratios of the 18/28 S rRNA are shown. Results represent one of two independent experiments with similar results. *D,* total RNA from MCF-7 cells transfected with mock, control siRNA (siNEG), or siRNA targeting WDR3 was analyzed by Northern blotting 72 h post-transfection using 28 and 18 S rRNA probes. The ratios of the 18/28 S rRNA are shown. The *graph* represents fold change in 18/28 S rRNA levels relative to mock-treated cells from three independent experiments ($p = 0.05$, Student's *t* test). *E,* total RNA from siRNA-transfected U2OS cells was analyzed by S1 nuclease protection assay using a probe complementary to the first 40 nucleotides of 47 S pre-RNA, and total protein was analyzed for β-actin expression by Western blotting (*top panel*). pre-rRNA and β-actin signals were quantified from triplicate samples using Aida software, and the levels of pre-rRNA were normalized to β-actin levels and expressed as a percentage from the highest signal (set at 100%) (*bottom panel*).

AC-15 (Abcam). Membranes were washed with TBS-T and incubated with IRdye-conjugated secondary antibodies (LI-COR Biosciences, Cambridge, UK), and protein was detected using Odyssey Image scanner system (LI-COR). Alternatively, membranes were incubated with horseradish peroxidase-conjugated secondary antibodies (Jackson ImmunoResearch), and immunocomplexes on the blots were detected by chemiluminescence (ECL Plus, GE Healthcare). Co-immunoprecipitation of the MDM2-rpL11 complex was carried out as described previously (14).

Quantitative and Semi-quantitative RT-PCR—Total RNA from R^+ and MCF-7 cells was isolated using TRIzol (Invitrogen) according to the manufacturer's instructions, and cDNA was synthesized by reverse transcription using 2 μg of RNA and Moloney murine leukemia virus reverse transcriptase kit (Invitrogen). For semi-quantitative RT-PCR, equal amounts of cDNA were amplified using HotStar *Taq*DNA polymerase (Qiagen, Germany) with WDR3-specific primers, *NEP1*-specific primers, β_2-microglobulin (*β2M*) primers, or *GAPDH* primers. Primer sequences were as follows: Mouse *wdr3*, 5′-TGCATCTAGCTGTTGGCTATGAGGATGGAG-3′ and 5′-CCTGTCTTGTCCACGGCGAGGTTCACAACT-3′; human *WDR3*, 5′-ATGCCTCGAGATATGGGGCTCACCAAGCAGTA-3′ and 5′-ATGCAAGCTTGTCGACTGCAAGGTTTACAAC-3′; mouse *nep1*, 5′-ATGTCTGCGGCCAGTGGTGGCT-3′ and 5′-TCAAATGACACCCCATACTT-3′; human *NEP1*, 5′-ATGGCCGCGCCCAGTGATGGAT-3′ and 5′-TCAAATGACCCCCCATACTT-3′; *β2M*, 5′-CCAGCAGAGAATGGAAAGTC-3′ and 5′-CCTCCATGATGCTGCTTACA-3′; *GAPDH*, 5′-ACCACAGTCCATGCCATCAC-3′ and 5′-TCCACCACCCTGTTGC-3′. For quantitative RT-PCR, equal amounts of cDNA were amplified using QuantiTect SYBR Green PCR kit (Qiagen) with WDR3 and β_2-microglobulin primers.

Cell Size and Cell Cycle Analysis by Flow Cytometry—Cells were removed from culture dishes with trypsin, resuspended in phosphate-buffered saline, and were analyzed (10,000 cells from triplicate samples) by fluorescence-activated cell sorting using CellQuest software (BD Biosciences) to obtain the mean forward scatter height (FSC-H).

For cell cycle analysis, cells were removed from culture dishes and resuspended in ice-cold phosphate-buffered saline containing 200 μg/ml RNase A (Sigma). Prior to analysis by fluorescence-activated cell sorting, Nonidet P-40 and propidium iodide were added to a final concentration of 0.1% and

50 μg/ml, respectively. DNA content was measured in the FL2 channel using CellQuest software (BD Biosciences). Cell viability was assessed by the uptake of propidium iodide using flow cytometry as described above.

Proliferation and Plating Efficiency Assay—Equal numbers of mock, control siRNA-(siNEG), or siRNA WDR3-transfected cells were cultured post-siRNA transfection for 24, 48, 72, or 96 h, then fixed in 96% ethanol, and stained with 0.05% crystal violet. Crystal violet staining was quantified using the Odyssey Image scanner system and normalized to the amount of staining on the 1st day of culture.

To assess plating efficiency, mock, control siRNA-(siNEG), or siRNA WDR3-transfected cells were plated in triplicate wells of a 6-well plate 24 h post-siRNA transfection, at a density of 500 cells per well, and cultured in complete media for 10 days. Cells were fixed in 96% ethanol and stained with 0.05% crystal violet. The numbers of colonies formed in each well were then counted.

RESULTS

IGF-I Induces the mRNA Expression of WDR3 and NEP1—In a cDNA screen for genes differentially expressed in R^- cells (mouse embryonic fibroblast cell line derived from IGF-IR knock-out mouse) and R^+ cells (R^- cells overexpressing the IGF-IR) (21), we identified genes encoding several ribosome-related proteins, including two proteins whose homologues are required for 40 S ribosome biogenesis in yeast, *WDR3* (accession number NM_175552), and *NEP1* (accession number NM_013536). To determine whether *WDR3* and *NEP1* expression were induced by IGF-I, R^+ cells were serum-starved, stimulated with IGF-I, and assessed for mRNA expression by semi-quantitative RT-PCR. *wdr3* mRNA accumulated 4, 8, and 12 h after IGF-I stimulation (supplemental Fig. S1*A*), although only a slight increase in *nep1* mRNA was observed after 4 and 6 h of IGF-I stimulation in R^+ cells (supplemental Fig. S1*B*). Northern blot analysis revealed that *WDR3* mRNA expression was also induced 4, 8, and 12 h post-IGF-I stimulation in the well characterized IGF-I-responsive tumor cell line, MCF-7 (Fig. 1*A*). Quantitative RT-PCR analysis also confirmed induction of *WDR3* mRNA using a lower IGF concentration (10 ng/ml) in MCF-7 cells (supplemental Fig. S1*C*). Similarly, *NEP1* mRNA was found to be more highly expressed 4, 8, and 12 h post-IGF-I stimulation by semi-quantitative RT-PCR (Fig. 1*B*).

We next analyzed the downstream signaling pathways activated by the IGF-IR that may be required for induction of *WDR3* and *NEP1*. MCF-7 cells stimulated with IGF-I were pretreated with pharmacological inhibitors of the phosphatidylinositol 3-kinase (PI3K) (LY294002), mammalian target of rapamycin (mTOR) (rapamycin), or mitogen-activated protein kinase (MAPK)/extracellular signal-regulated kinase (ERK) kinase (MEK1) (PD98059) signaling pathways. *WDR3* and *NEP1* mRNA expression were assessed by semi-quantitative RT-PCR. Induction of *WDR3* mRNA by IGF-I was suppressed by inhibitors of the PI3K/mTOR pathway (Fig. 1*C*), although the MEK1 inhibitor PD98059 had no effect. Similarly, the induction of *NEP1* mRNA by IGF-I was suppressed by PI3K inhibition, although rapamycin and PD98059 had no effect (Fig. 1*D*). These data indicate that PI3K and mTOR activity are necessary for IGF-I-mediated induction of *WDR3* mRNA, but only PI3K activity is required for induction of *NEP1* mRNA.

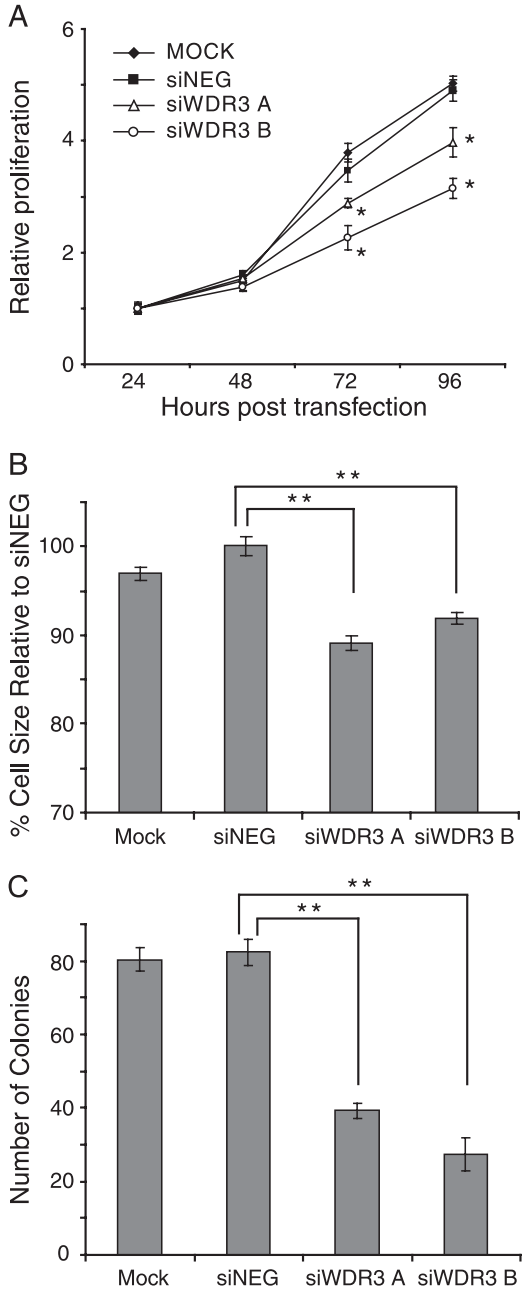

FIGURE 3. **Suppression of WDR3 results in reduced cell proliferation, cell size, and foci formation.** *A*, MCF-7 cells were mock-transfected, transfected with control siRNA, or siRNA targeting WDR3 for 24 h and then seeded at equal numbers in complete media cultures. Cell density was monitored by crystal violet staining for up to 96 h post-transfection. The data represent an average of 6 wells from a representative experiment (*, $p < 0.001$, Student's *t* test). *B*, cells transfected as in *A* were assessed for cell size 72 h post-siRNA transfection using the mean FSC-H signal on a flow cytometer as a measure of relative cell size. Data represent an average of the mean FSC-H from five independent samples and graphed as change in percentage cell size relative to control siRNA-transfected cells (siNEG) (**, $p < 0.001$, Student's *t* test). *C*, MCF-7 cells were mock-transfected and transfected with control siRNA, or WDR3 siRNA for 24 h. Cells were seeded at a density of 500 cells per well of a 6-well plate in complete media for 10 days, at which time cells were stained with crystal violet. The number of colonies formed were counted and presented as the mean ± S.D. of colonies per well from triplicate samples (**, $p < 0.001$, Student's *t* test).

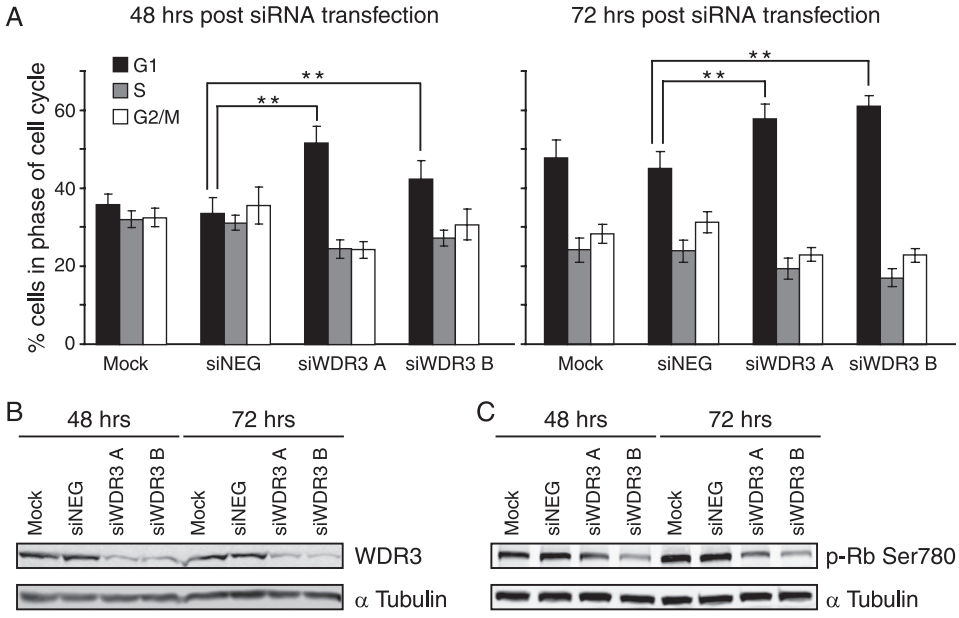

FIGURE 4. **Suppression of WDR3 results in an accumulation of cells in the G_1 phase of the cell cycle.** *A,* cell cycle profiles of MCF-7 cells that were mock-transfected, transfected with control siRNA, or siRNA targeting WDR3 were stained with propidium iodide. DNA content was analyzed by flow cytometry 48 h (*left panel*) and 72 h (*right panel*) post-transfection. *Graphs* indicate the percentages of cells in G_1 (*black*), S (*gray*), and G_2/M (*white*) phases of the cell cycle from triplicate samples for three separate experiments (**, $p < 0.001$, Student's *t* test). *B,* levels of WDR3 protein expression are shown with α-tubulin as a loading control. Results represent one of three independent experiments with similar results. *C,* phosphorylation of Rb at serine 780 was analyzed by Western blotting at 48 and 72 h post-transfection. α-Tubulin is shown as a loading control. Results represent one of three independent experiments with similar results.

Because little is known about WDR3 function in mammalian cells and because it is located on a region of chromosome 1 (1p12-13) disrupted in malignancies and solid tumors (26), we focused our subsequent studies on this gene. WDR3 protein expression was examined by Western blotting in R^- and R^+ cells using antisera raised against a peptide corresponding to an amino acid sequence of the protein. WDR3 protein was more highly expressed in R^+ cells than R^- cells (Fig. 1, *E*, *left panel,* and *F*). Induction of WDR3 protein in response to IGF-I was not evident, and WDR3 protein was not altered by exposure of cells to cycloheximide for up to 48 h, suggesting that WDR3 is a very stable protein. WDR3 protein was also found to be more highly expressed in the transformed Rat-1/Myc cells compared with Rat-1 cells (Fig. 1, *E*, *right panel,* and *F*), supporting previous reports in which *WDR3* mRNA expression was shown to be enhanced by c-Myc (34). Overall, these results indicate that WDR3 is more abundant in cells transformed by overexpression of the IGF-IR or c-Myc.

WDR3 Is Required for Processing of 18 S rRNA—The yeast homologue of WDR3, Utp12, has been implicated in the processing of 18 S rRNA (28). More recently, WDR3 was identified as a component of an 80 S U3 small nucleolar ribonucleoprotein complex involved in pre-rRNA processing of the small ribosomal subunit (35), but its function in this complex is still unknown. To investigate the function of WDR3 in rRNA processing of mammalian cells, we first suppressed its expression in two cell lines that are responsive to IGF-I and express functional p53 (MCF-7 and the osteosarcoma cell line U2OS) using siRNA. Two oligonucleotides (siWDR3 A and siWDR3 B) specifically targeting WDR3 reduced the expression of WDR3 protein by ~85 and 90%, respectively, when compared with mock or control siRNA-transfected cells (siNEG) by 72 h post-siRNA transfection (Fig. 2*A*).

To assess rRNA processing we investigated the levels of rRNA species in cells with suppressed WDR3. Northern blots representing total RNA were probed with sequences complementary to precursor and mature rRNA species, namely human ITS-1 (internal transcribed spacer), ITS-2, and 28 and 18 S rRNA within the primary 47 S rRNA transcript (Fig. 2*B*). Hybridization of the ITS-1 probe indicated an accumulation of 34 S pre-rRNA upon suppression of WDR3 compared with control siRNA-transfected cells (Fig. 2*C*). Furthermore, a reduction of a downstream 21 S pre-rRNA intermediate was detected upon suppression of WDR3 compared with controls. Precursors of the 5.8 or 28 S rRNA (12 and 32 S rRNA, respectively) were unaffected by suppression of WDR3 protein. Hybridization with probes specific for 18 and 28 S rRNA indicated a marked reduction in the production of mature 18 S rRNA upon suppression of WDR3 protein with no change in 28 S rRNA. Similarly the levels of 18 S rRNA in MCF-7 were reduced by suppression of WDR3, but no change in 28 S rRNA production was detected (Fig. 2*D*).

We also determined the levels of pre-rRNA in cells by analyzing total cellular RNA (greater than 200 bp) in S1 nuclease protection assays (Fig. 2*E*). No significant difference was observed in pre-rRNA levels upon suppression of WDR3 compared with controls at 24 h post-siRNA transfection. However, both siWDR3 A- and siWDR3 B-transfected cells exhibited a 1.5–2-fold decrease in pre-rRNA levels after 48 h siRNA transfection (Fig. 2*E*, *bottom panel, gray bars*). Interestingly, at 72 h post-siRNA transfection, cells with suppressed WDR3 contained higher levels of pre-rRNA compared with controls (Fig. 2*E*, *bottom panel, white bars*). This increase is likely due to an accumulation of the 47 S rRNA caused by defects in rRNA processing in cells lacking WDR3.

Because IGF-I stimulation leads to increased levels of WDR3 mRNA (this study) and also to the activation of rRNA synthesis (15–17), we next sought to determine whether WDR3 may also regulate rRNA synthesis by investigating the effect of WDR3 suppression on the activity of pol I transcription machinery using *in vitro* transcription assay. No changes in the specific activity of nuclear extracts from U2OS cells transfected with either control or WDR3-specific siRNA were observed at 48 h (supplemental Fig. S2*A*, *right panel, black bars*). However, at 72 h post-siRNA transfection, the specific activity of nuclear extracts from cells with suppressed WDR3 was detectably

lower than controls (supplemental Fig. S2*A*, *right panel, gray bars*). Although no major decrease in the levels of pol I subunits RPA135 and PAF53 were observed after WDR3 depletion (supplemental Fig. S2*B*), the catalytic (nonspecific) activity of pol I was also decreased in nuclear extracts from cells with suppressed WDR3 but only 72 h after transfection (supplemental Fig. S2*C*, *gray bars*). These data suggest that cells with suppressed WDR3 exhibit a slightly lower rRNA synthesis capacity. However, it is unclear whether WDR3 can directly regulate pol I transcription or whether its suppression leads to activation of another regulatory pathway that down-regulates pol I activity (such as p53). Overall, these results demonstrate that WDR3 is required for efficient processing of 18 S rRNA in mammalian cells and are consistent with studies in yeast showing that the WDR3 homologue Utp12 is required for rRNA processing of the small ribosome subunit (28).

WDR3 Suppression Reduces Cell Proliferation, Cell Size, and Foci Formation—Given that ribosome biogenesis, cell growth, and cell proliferation are tightly linked, we next investigated the effect of suppressing WDR3 protein on cell proliferation and cell size. MCF-7 cells with suppressed WDR3 expression showed a 35% decrease in proliferation rate compared with control siRNA-transfected cells (Fig. 3*A*). Moreover, WDR3 depletion led to an 8–10% decrease in cell size as determined by flow cytometry using the mean forward scatter height (FSC-H) value as a measure of relative cell size (Fig. 3*B*).

To determine whether WDR3 plays a role in the proliferation of transformed cells, we performed plating efficiency assays, which measure the ability of cells to form foci in low density cultures. MCF-7 cells with suppressed WDR3 exhibited a marked reduction in the number of foci compared with controls (Fig. 3*C*). Taken together, these data indicate that WDR3 enhances the growth and proliferation of transformed cells.

Suppression of WDR3 Results in Cell Cycle Arrest in the G_1 Phase of the Cell Cycle—We next investigated whether the effects of suppressing WDR3 on cell growth were due to differences in cell viability or cell cycle progression. Cell viability and cell cycle profiles were analyzed using flow cytometry 48 and 72 h after transfection with siRNA. There was no morphological evidence of cell death/apoptosis in the cultures and no change in propidium iodide uptake in cells with WDR3 expression suppressed compared with controls (supplemental Fig. S3), which indicates no cell death was occurring. However, suppression of WDR3 resulted in an increased accumulation of cells in the G_1 phase of the cell cycle compared with controls (Fig. 4*A*), which indicates a G_1 cell cycle arrest. The number of cells in the G_1 phase of the cell cycle was increased by 10–18% following suppression of WDR3 for 48 and 72 h. This correlated with a decrease in the number of cells in the S and G_2 phases of the cell cycle (Fig. 4*A*). Expression levels of WDR3 protein are shown in Fig. 4*B*.

Phosphorylation of Rb at serine 780 is necessary for cycling cells to enter the S phase of the cell cycle (36). Cells with suppressed WDR3 exhibited a marked reduction in the levels of phosphorylation of Rb at serine 780 compared with controls (Fig. 4*C*), which confirms they are unable to pass the G_1/S phase checkpoint, thus they accumulate in the G_1 phase of the cell cycle.

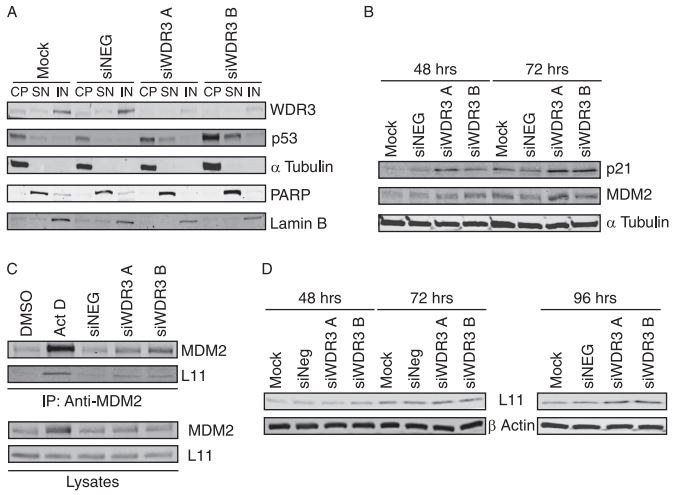

FIGURE 5. **Suppression of WDR3 results in activation of the p53 stress response pathway.** *A,* U2OS cells were mock-transfected, transfected with control siRNA, or siRNA targeting WDR3 for 72 h. Subcellular fractions were prepared for cytoplasmic (*CP*), soluble nuclear (*SN*), and insoluble nuclear (*IN*) fractions. Expression of WDR3, p53, and α-tubulin as a marker for the cytoplasmic fraction, poly(ADP-ribose) polymerase as a marker for the soluble nuclear fraction, and lamin B as a marker for the insoluble nuclear fraction were determined by Western blotting. Results represent one of three independent experiments with similar results. *B,* U2OS cells mock-transfected, transfected with control siRNA, or siRNA targeting WDR3 for 48 and 72 h were analyzed by Western blot for expression of p21 and MDM2. α-Tubulin is shown as a loading control. Results represent one of three independent experiments with similar results. *C,* U2OS cells were transfected with control siRNA or siRNA targeting WDR3 for 48 h or were exposed to 10 ng/ml actinomycin D (*Act D*) or DMSO vehicle control for 10 h prior to immunoprecipitation (*IP*) with anti-MDM2 antibody. MDM2 and rpL11 levels present in immunoprecipitations were analyzed by Western blotting (*top panel*). The levels of MDM2 and rpL11 present in lysates are shown (*bottom panel*) and represent 20% of total lysate input used in immunoprecipitations. Results represent one of three independent experiments with similar results. *D,* U2OS cells mock-transfected, transfected with control siRNA, or siRNA targeting WDR3 were analyzed for rpL11 protein expression after 48, 72, and 96 h. β-Actin is shown as a control for loading. Results represent one of three independent experiments with similar results.

p53 Stress Response Pathway Is Activated upon Suppression of WDR3—It has previously been demonstrated that cross-talk between ribosome biogenesis and cell cycle regulation is mediated by stabilizing the tumor suppressor protein p53 (8, 37, 38). Since depletion of WDR3 leads to defects in 18 S rRNA processing, we next investigated whether p53 is involved in the cell cycle arrest induced by WDR3 suppression. We first determined p53 protein levels in the subcellular fractions of U2OS cells. Compared with control cells, in which p53 is present at low levels and primarily in the cytosolic fraction (Fig. 5*A*), both siWDR3 A- and siWDR3 B-transfected cells exhibited increased p53 expression in the cytoplasmic fractions and an accumulation of p53 in the soluble nuclear fractions. To determine whether the increase in p53 levels correlates with p53 transcriptional activity, we analyzed the expression of proteins encoded by p53-responsive genes, $p21^{WAF1/CIP1}$ and *MDM2*. Both p21 and MDM2 protein levels were increased in U2OS cells with suppressed WDR3 expression (Fig. 5*B*), indicating that both p53 levels and activity are increased upon suppression of WDR3. Similar results were observed in MCF-7 cells (supplemental Fig. S4), which like U2OS cells do not express p14ARF, suggesting that the activation of p53 upon suppression of WDR3 is ARF-independent.

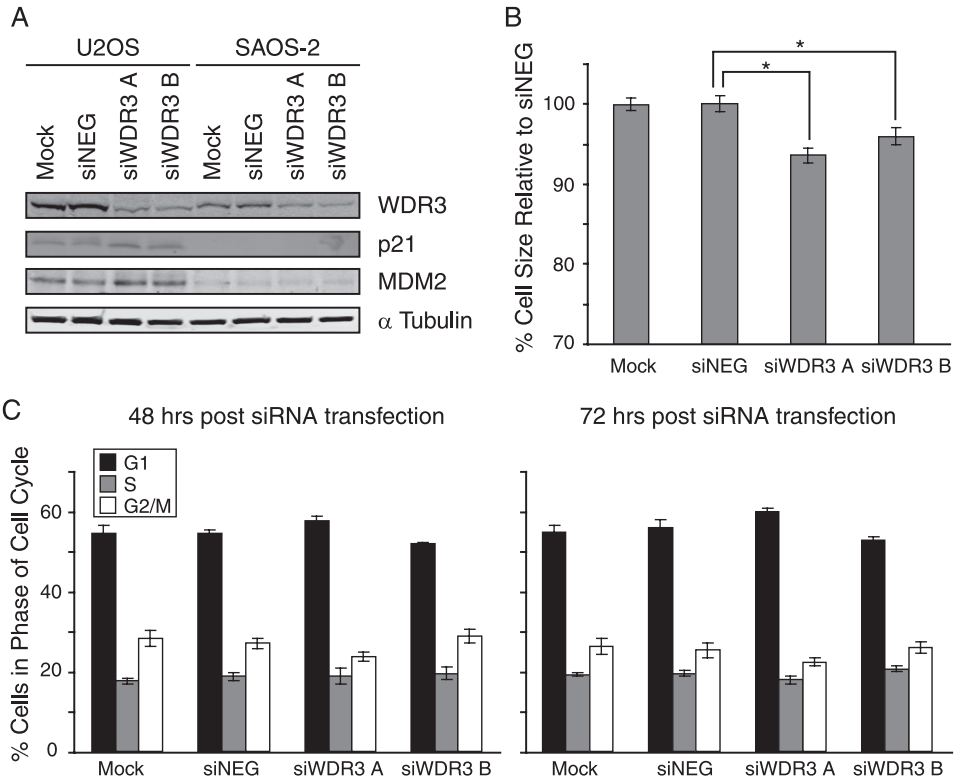

FIGURE 6. **Cell cycle arrest due to suppression of WDR3 does not occur in cells deficient in Rb and p53.** *A*, U2OS and SAOS-2 cells were mock-transfected, transfected with control siRNA, or siRNA targeting WDR3 and then analyzed for expression of WDR3, p21, MDM2, and α-tubulin by Western blot. Results represent one of three independent experiments with similar results. *B*, SAOS-2 cells transfected as in *A* for 72 h were assessed for cell size using the mean FSC-H signal on a flow cytometer. Data represent an average of the mean FSC-H from six independent samples and graphed as change in percentage cell size relative to control siRNA-transfected cells (siNEG) (*, $p < 0.05$, Student's *t* test). *C*, cell cycle profiles of SAOS-2 cells mock-transfected, transfected with control siRNA, or siRNA targeting WDR3 were stained with propidium iodide, and DNA content was analyzed by flow cytometry at 48 h (*left panel*) and 72 h (*right panel*) post-transfection. *Graphs* indicate the percentages of cells in G_1 (*black*), S (*gray*), and G_2/M (*white*) phases of the cell cycle from triplicate samples of three independent experiments.

Defects in ribosome biogenesis can lead to reduced degradation of p53 by the proteasome via an MDM2-dependent pathway (10) that causes stabilization and accumulation of p53. In U2OS cells, we observed that steady-state levels of p53 increased when WDR3 was suppressed (time 0 h, supplemental Fig. S5). Moreover, exposure of cells to the proteasome inhibitor MG132 causes an accumulation of p53 protein in control cells with little change in p53 levels in cells with suppressed WDR3, suggesting that in these cells p53 is already stabilized and is not targeted for proteasomal degradation.

Stabilization of p53 upon impairment of ribosome synthesis has been linked to increased binding of free (nonribosomal) rpL11 to MDM2 (14, 37). We observed increased levels of rpL11 co-immunoprecipitating with MDM2 from cells with suppressed WDR3 for 48 h compared with controls (Fig. 5*C*). Actinomycin D, which has previously been reported to increase the rpL11-MDM2 interaction (10, 39), was used as a positive control. MDM2 levels were moderately increased in cells with suppressed WDR3 (Fig. 5*B*), which could potentially lead to increased MDM2-rpL11 interactions. However, it has been shown previously that the mere stabilization of MDM2 without nucleolar stress does not induce the rpL11 binding to MDM2 (39). In addition, no change in steady-state levels of rpL11 expression were detected 48 or 72 h after siRNA transfection (Fig. 5*D*).

However, rpL11 expression increased over longer periods of WDR3 suppression (96 h after transfection), which is consistent with reports that rpL11 is up-regulated upon impairment of 40 S ribosome biogenesis (14). Overall, the data indicate that defects in ribosome biogenesis caused by depletion of WDR3 lead to increased rpL11 binding to MDM2, which results in the activation of a p53-dependent stress response pathway.

Suppression of WDR3 Protein in SAOS-2 Cell Does Not Result in Cell Cycle Arrest—To further investigate whether p53 is required for cell cycle arrest upon WDR3 suppression, we compared the effects of WDR3 depletion in U2OS and MCF-7 cells that express wild-type p53 with two cell lines that are deficient in p53 (SAOS-2, human osteosarcoma cell line, and HeLa cells). In U2OS cells (Fig. 5*B*), depletion of WDR3 leads to up-regulation of p21 and MDM2 expression. In contrast, depletion of WDR3 has no effect on p21 or MDM2 protein levels in SAOS-2 cells (Fig. 6*A*), confirming that p53 is necessary for the regulation of these proteins. Similarly, no increases in p53, p21, or MDM2 levels were observed in HeLa cells when compared with MCF-7 cells (supplemental Fig. S4*B*). Moreover, WDR3 suppression in SAOS-2 cells had no effect on cell cycle distribution (Fig. 6*C*) when compared with cells containing wild-type p53 (Fig. 4*A*). HeLa cells also exhibited no change in cell cycle distribution when WDR3 was suppressed (supplemental Fig. S6). These data indicate that the cell cycle arrest provoked by the impairment of 18 S rRNA synthesis upon suppression of WDR3, is due to activation of a p53-dependent G_1 cell cycle checkpoint.

To determine whether p53 is required for the reduction in cell size upon suppression of WDR3 (Fig. 3*B*), SAOS-2 cells were assessed for size 72 h after transfection with siRNA. A slight reduction in size was observed in cells transfected with siWDR3 A or siWDR3 B compared with controls (Fig. 6*B*) that is within 3–4% less than that observed in cells containing wild-type p53 (Fig. 3*B*). This suggests that the reduction in cell size in WDR3-depleted cells is, at least in apart, independent of p53. Taken together, the data indicate that suppression of WDR3 does not result in the accumulation of MDM2 and p21 proteins or result in G_1 phase cell cycle arrest in p53-deficient SAOS-2 cells. This suggests that p53 is the key regulator of cell cycle

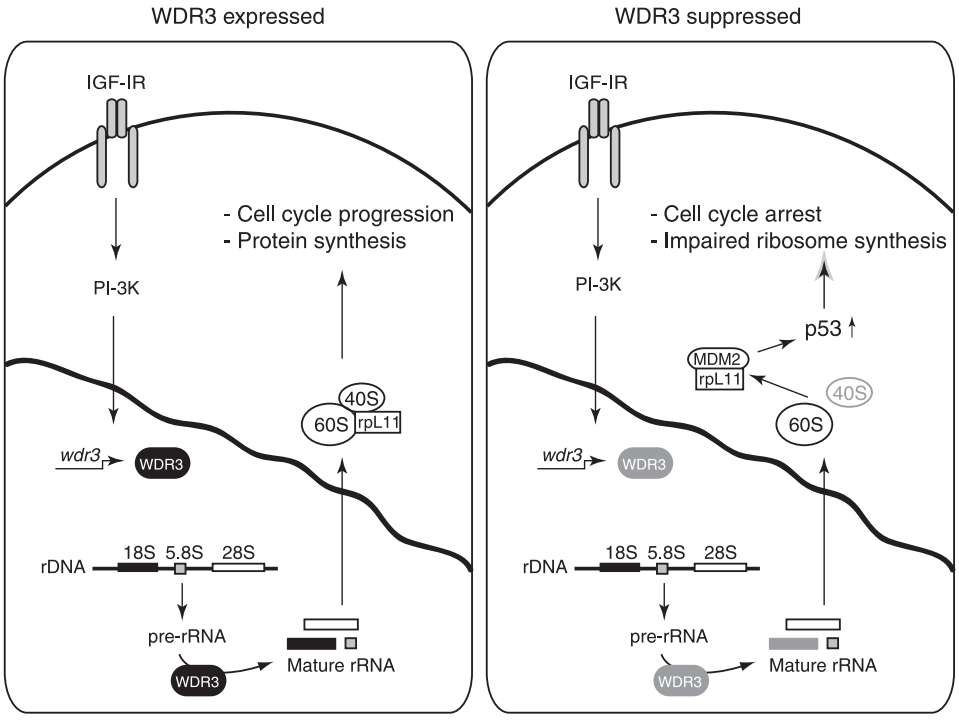

FIGURE 7. **Model illustrating the role of WDR3 in mediating cross-talk between ribosome biogenesis and p53-mediated cell cycle regulation.** In cells expressing WDR3 (*left panel*), *WDR3* gene expression is induced by the IGF-I signaling pathway, and the protein is localized to the nucleus where it is required for pre-rRNA processing of 18 S rRNA. Under these conditions, protein synthesis and cell cycle progression occur. In cells with suppressed WDR3 (*right panel*), defects in 18 S rRNA synthesis occur resulting in impaired 40 S ribosome biogenesis. As a result of impaired ribosome biogenesis (ribosomal stress), free rpL11 binds MDM2 allowing stabilization of p53. Under these conditions of impaired ribosome synthesis, p53 triggers cell cycle arrest at the G_1/S checkpoint.

progression in response to the disturbance of ribosome biogenesis by depletion of WDR3.

DISCUSSION

Ribosome biogenesis and cell cycle regulation are two tightly coordinated cellular processes necessary for cell proliferation and survival. In this study, we show for the first time that WDR3 is an IGF-I-responsive gene involved in ribosome biogenesis and p53-mediated cell cycle regulation in mammalian cells (summarized in model in Fig. 7). Our findings also support other studies (7, 40) indicating that cross-talk exists between impairment of ribosome biogenesis and p53-dependent cell cycle arrest that serves to protect cells from replicating in unfavorable conditions. *WDR3* is also a new transcriptional target of the IGF-I signaling pathway that is directly involved in ribosome synthesis, which is consistent with the essential function of IGF-IR signaling in cell growth.

The IGF-IR can regulate cell growth and differentiation by controlling transcription of rRNA by RNA pol I (15). Thus, it controls the rate of ribosome synthesis, protein turnover, and cell growth. WDR3 and NEP1 were among several ribosome-related proteins expressed more highly in cells overexpressing the IGF-IR compared with IGF-IR null cells. These included ribosomal proteins involved in the assembly of the small (rpS21, rpS24, and rpS26) and large (rpL3, rpL7, rpL10a, rpL35a, and rpL37a) ribosomal subunits (21). *WDR3* and *NEP1* mRNA were induced within a few hours of IGF-I stimulation suggesting that these genes are rapidly transcribed in response to IGF-I. This induction is dependent on the activity of the PI3K and mTOR pathway, whose activity is essential for ribosome processing and expression of ribosomal proteins, including rpS6 (41). The PI3K/mTOR pathway also plays a central role in RNA pol I activation in response to IGF-I (17). WDR3 and NEP1 homologues in yeast are essential for processing 18 S rRNA (23, 28). Thus, overall IGF-I signaling regulates ribosome biogenesis not only by controlling the rate of rRNA transcription by pol I (15) but also through the induction of structural proteins (21) and ribosome processing factors such as WDR3 and NEP1.

In this study we chose to focus on the WD repeat protein WDR3, as this gene is located on chromosome 1p12-p13 (25), a region of chromosome 1 that is associated with many cancers. Individuals bearing a single nucleotide polymorphism (SNP) in the *WDR3* gene locus have a strong association with thyroid cancer susceptibility (42). Deletions of the *WDR3* gene locus have been detected in many malignant solid tumors of epithelial origin (26), and the unbalanced translocation t(1;3)(p12–13;q11) of the *WDR3* locus has been detected in several brain tumors (43). These data strongly suggest that WDR3 may be implicated in cancer development. Our findings indicate that WDR3 is more highly expressed in cells overexpressing the IGF-IR and the proto-oncogene c-*myc*, another well characterized regulator of ribosome synthesis and cell growth (6). Thus, WDR3 may be a common mediator of IGF-IR and Myc action in transformed cells. Our observation that suppression of WDR3 in the breast carcinoma cell line MCF-7 reduced cell proliferation, decreased cell size, and reduced foci formation indicates that WDR3 confers a growth and proliferative advantage on cancer cells.

Mammalian WDR3 is a component of the 80 S complex of the small subunit processome, implicated in the 40 S ribosome synthesis pathway (35). Here, we show that WDR3 is necessary for processing of 18 S rRNA, the main RNA component of the small 40 S ribosome subunit. WDR3 is therefore a functional homologue of the yeast Utp12 protein. Interestingly, suppression of WDR3 also leads to a moderate down-regulation of pol I activity. This effect is most likely secondary to the role of WDR3 in 18 S rRNA processing and is likely caused by the activation of p53, which has previously been demonstrated to repress pol I transcription activity (44). Several WD40 repeat proteins, including Bop1, WDR12, and WDR36, have recently been associated with ribosome synthesis and cell proliferation (29, 45, 46). The exact mechanism of action of these WD repeat

proteins, including WDR3, is not known, but it is logical to propose that they may act as scaffolds for other proteins through interactions with their multiple WD40 protein-binding faces. We observed that WDR3 protein is redistributed within the nucleus when ribosome biogenesis is disrupted using low concentrations of actinomycin D (supplemental Fig. S7). This is in agreement with reports indicating that nucleolar proteins required for ribosome biogenesis move within the nucleus under varying stress conditions (47).

The nucleolus has been described as a stress sensor that maintains p53 at low levels. Inhibition of ribosome biogenesis leads to accumulation of p53, in the presence or absence of nucleolar disruption (9, 14, 37). Here, upon suppression of WDR3 we observed stabilization of p53 in response to impaired ribosome biogenesis. Accumulation of p53 in conditions of nucleolar stress occurs by inhibition of its degradation mediated by MDM2 (48). Sequestration of MDM2 and activation of p53 involve the tumor suppressor protein p14ARF and ribosomal proteins, including rpL5, rpL11, or rpL23 (12, 39, 49). In this study we used cell lines that do not express the p14ARF protein. Therefore, we can conclude that the induction of p53 upon WDR3 suppression is an ARF-independent process. We investigated the involvement of ribosomal protein L11 because it has recently been identified as a negative regulator of MDM2 upon impairment of 40 S ribosome synthesis (14). Suppression of WDR3 resulted in increased binding of rpL11 to MDM2, which leads to a p53-dependent G_1 cell cycle arrest (Fig. 7). Our results demonstrate that 40 S ribosome biogenesis is tightly coordinated with cell cycle progression through regulation of MDM2/p53 signaling and are consistent with a role for rpL11 as a key mediator in the cellular response to impaired ribosome biogenesis due to defective 18 S rRNA processing.

In conclusion, our study has shown that IGF-IR signaling controls ribosome biogenesis by regulating the expression of proteins directly involved in the processing of ribosomal subunits and that this is integrated with p53-mediated regulation of cell cycle progression. We propose that deregulated expression of WDR3 in cancer cells would disrupt the signaling pathways that exist between ribosome biogenesis and p53 activation. Thus, increased expression of WDR3 would promote cell proliferation, especially in tumor cells where p53 is mutated or not expressed.

Acknowledgments—We are grateful to our colleagues in the Cell Biology Laboratory for helpful discussions, to Gary Loughran for advice on RNA, and to Kurt Tidmore for preparing illustrations.

REFERENCES

1. Pardee, A. B. (1989) *Science* **246,** 603–608
2. Thomas, G. (2000) *Nat Cell Biol.* **2,** E71–E72
3. Moss, T., and Stefanovsky, V. Y. (1995) *Prog. Nucleic Acids Res. Mol. Biol.* **50,** 25–66
4. Schnapp, A., Pfleiderer, C., Rosenbauer, H., and Grummt, I. (1990) *EMBO J.* **9,** 2857–2863
5. Mayer, C., and Grummt, I. (2006) *Oncogene* **25,** 6384–6391
6. Schmidt, E. V. (1999) *Oncogene* **18,** 2988–2996
7. Pestov, D. G., Strezoska, Z., and Lau, L. F. (2001) *Mol. Cell. Biol.* **21,** 4246–4255
8. Ma, H., and Pederson, T. (2007) *Mol. Biol. Cell* **18,** 2630–2635
9. Rubbi, C. P., and Milner, J. (2003) *EMBO J.* **22,** 6068–6077
10. Lohrum, M. A., Ludwig, R. L., Kubbutat, M. H., Hanlon, M., and Vousden, K. H. (2003) *Cancer Cell* **3,** 577–587
11. Weber, J. D., Taylor, L. J., Roussel, M. F., Sherr, C. J., and Bar-Sagi, D. (1999) *Nat. Cell Biol.* **1,** 20–26
12. Dai, M. S., Zeng, S. X., Jin, Y., Sun, X. X., David, L., and Lu, H. (2004) *Mol. Cell. Biol.* **24,** 7654–7668
13. Chen, D., Zhang, Z., Li, M., Wang, W., Li, Y., Rayburn, E. R., Hill, D. L., Wang, H., and Zhang, R. (2007) *Oncogene* **26,** 5029–5037
14. Fumagalli, S., Di Cara, A., Neb-Gulati, A., Natt, F., Schwemberger, S., Hall, J., Babcock, G. F., Bernardi, R., Pandolfi, P. P., and Thomas, G. (2009) *Nat. Cell Biol.* **11,** 501–508
15. Tu, X., Batta, P., Innocent, N., Prisco, M., Casaburi, I., Belletti, B., and Baserga, R. (2002) *J. Biol. Chem.* **277,** 44357–44365
16. Wu, A., Tu, X., Prisco, M., and Baserga, R. (2005) *J. Biol. Chem.* **280,** 2863–2872
17. James, M. J., and Zomerdijk, J. C. (2004) *J. Biol. Chem.* **279,** 8911–8918
18. Sell, C., Rubini, M., Rubin, R., Liu, J. P., Efstratiadis, A., and Baserga, R. (1993) *Proc. Natl. Acad. Sci. U.S.A.* **90,** 11217–11221
19. Sell, C., Dumenil, G., Deveaud, C., Miura, M., Coppola, D., DeAngelis, T., Rubin, R., Efstratiadis, A., and Baserga, R. (1994) *Mol. Cell. Biol.* **14,** 3604–3612
20. Floyd, S., Favre, C., Lasorsa, F. M., Leahy, M., Trigiante, G., Stroebel, P., Marx, A., Loughran, G., O'Callaghan, K., Marobbio, C. M., Slotboom, D. J., Kunji, E. R., Palmieri, F., and O'Connor, R. (2007) *Mol. Biol. Cell* **18,** 3545–3555
21. Loughran, G., Huigsloot, M., Kiely, P. A., Smith, L. M., Floyd, S., Ayllon, V., and O'Connor, R. (2005) *Oncogene* **24,** 6185–6193
22. O'Callaghan, K. M., Ayllon, V., O'Keeffe, J., Wang, Y., Cox, O. T., Loughran, G., Forgac, M., and O'Connor, R. (2010) *J. Biol. Chem.* **285,** 381–391
23. Eschrich, D., Buchhaupt, M., Kötter, P., and Entian, K. D. (2002) *Curr. Genet.* **40,** 326–338
24. Liu, P. C., and Thiele, D. J. (2001) *Mol. Biol. Cell* **12,** 3644–3657
25. Claudio, J. O., Liew, C. C., Ma, J., Heng, H. H., Stewart, A. K., and Hawley, R. G. (1999) *Genomics* **59,** 85–89
26. Mertens, F., Johansson, B., Höglund, M., and Mitelman, F. (1997) *Cancer Res.* **57,** 2765–2780
27. Smedley, D., Sidhar, S., Birdsall, S., Bennett, D., Herlyn, M., Cooper, C., and Shipley, J. (2000) *Genes Chromosomes Cancer* **28,** 121–125
28. Dragon, F., Gallagher, J. E., Compagnone-Post, P. A., Mitchell, B. M., Porwancher, K. A., Wehner, K. A., Wormsley, S., Settlage, R. E., Shabanowitz, J., Osheim, Y., Beyer, A. L., Hunt, D. F., and Baserga, S. J. (2002) *Nature* **417,** 967–970
29. Hölzel, M., Rohrmoser, M., Schlee, M., Grimm, T., Harasim, T., Malamoussi, A., Gruber-Eber, A., Kremmer, E., Hiddemann, W., Bornkamm, G. W., and Eick, D. (2005) *J. Cell Biol.* **170,** 367–378
30. Learned, R. M., Learned, T. K., Haltiner, M. M., and Tjian, R. T. (1986) *Cell* **45,** 847–857
31. Bell, S. P., Learned, R. M., Jantzen, H. M., and Tjian, R. (1988) *Science* **241,** 1192–1197
32. Panov, K. I., Friedrich, J. K., and Zomerdijk, J. C. (2001) *Mol. Cell. Biol.* **21,** 2641–2649
33. Tanaka, T., Grusby, M. J., and Kaisho, T. (2007) *Nat. Immunol.* **8,** 584–591
34. Schlosser, I., Hölzel, M., Mürnseer, M., Burtscher, H., Weidle, U. H., and Eick, D. (2003) *Nucleic Acids Res.* **31,** 6148–6156
35. Turner, A. J., Knox, A. A., Prieto, J. L., McStay, B., and Watkins, N. J. (2009) *Mol. Cell. Biol.* **29,** 3007–3017
36. Knudsen, E. S., and Wang, J. Y. (1997) *Mol. Cell. Biol.* **17,** 5771–5783
37. Barkiæ, M., Crnomarkoviæ, S., Grabusiæ, K., Bogetiæ, I., Paniæ, L., Tamarut, S., Cokariæ, M., Jeriæ, I., Vidak, S., and Volareviæ, S. (2009) *Mol. Cell. Biol.* **29,** 2489–2504
38. Hölzel, M., Orban, M., Hochstatter, J., Rohrmoser, M., Harasim, T., Malamoussi, A., Kremmer, E., Längst, G., and Eick, D. (2010) *J. Biol. Chem.* **285,** 6364–6370
39. Zhang, Y., Wolf, G. W., Bhat, K., Jin, A., Allio, T., Burkhart, W. A., and Xiong, Y. (2003) *Mol. Cell. Biol.* **23,** 8902–8912
40. Sulic, S., Panic, L., Barkic, M., Mercep, M., Uzelac, M., and Volarevic, S. (2005) *Genes Dev.* **19,** 3070–3082

41. Hannan, K. M., Brandenburger, Y., Jenkins, A., Sharkey, K., Cavanaugh, A., Rothblum, L., Moss, T., Poortinga, G., McArthur, G. A., Pearson, R. B., and Hannan, R. D. (2003) *Mol. Cell. Biol.* **23,** 8862–8877
42. Baida, A., Akdi, M., González-Flores, E., Galofré, P., Marcos, R., and Velázquez, A. (2008) *Cancer Epidemiol. Biomarkers Prev.* **17,** 1499–1504
43. Steilen-Gimbel, H., Niedermayer, I., Feiden, W., Freiler, A., Steudel, W. I., Zang, K. D., and Henn, W. (1999) *Genes Chromosomes Cancer* **26,** 270–272
44. Budde, A., and Grummt, I. (1999) *Oncogene* **18,** 1119–1124
45. Skarie, J. M., and Link, B. A. (2008) *Hum. Mol. Genet.* **17,** 2474–2485
46. Strezoska, Z., Pestov, D. G., and Lau, L. F. (2000) *Mol. Cell. Biol.* **20,** 5516–5528
47. Chen, D., and Huang, S. (2001) *J. Cell Biol.* **153,** 169–176
48. Honda, R., Tanaka, H., and Yasuda, H. (1997) *FEBS Lett.* **420,** 25–27
49. Marechal, V., Elenbaas, B., Piette, J., Nicolas, J. C., and Levine, A. J. (1994) *Mol. Cell. Biol.* **14,** 7414–7420